Opto-electronic systems for addressing Ru oxygen sensors: their design optimization and calibration process

(Invited Paper)

E.A.D Austin, J.P. Dakin

Optoelectronics Research Centre, University of Southampton, Southampton SO17 1BJ

ABSTRACT

The paper describes research at Southampton University, aimed at optimising the design of fibre-remoted dissolved-oxygen sensors, using immobilized fluorescent Ru^{2+} indicators. The design and construction of two types of fluorescence lifetime monitoring units, one type using phase-delay-monitoring and the other using photon-counting, is described. Results from a detailed theoretical study of a photon-counting RLD fluorescence lifetime sensor are presented, with specific attention to noise aspects. By numerical modeling of an analytical solution, the optimum time-window boundaries for the photon-counting system are identified. A surprising result is that the signal/noise can actually be improved by not using photon counts from all of the exponential decay, but leaving a time-gap in the measurement improves lifetime accuracy. Our previously reported Ti^{3+} - doped sapphire fluorescence-lifetime calibration probe is described, and a new method for RLD interrogator verification using the probe is demonstrated.

INTRODUCTION

Apart from its importance in natural environments, oxygen is a reactant in a huge number of chemical and biochemical processes. Accurately measuring the level of gaseous or dissolved oxygen has been the subject of extensive worldwide research. Oxygen determination, both in the gaseous phase and dissolved in solvents, is vital in areas such as environmental monitoring[1], chemical reaction analysis[2], and medical applications[3,4,5,6,7].

The optical oxygen sensor, which usually involves an Ru^{2+}-complex indicator, immobilised in a silicone or sol-gel matrix, has over the last ten years, become an increasingly popular alternative to traditional electro-chemical sensors, with increasing application in many environmental and clinical monitoring areas. The advantages most commonly identified are; no O_2 consumption in the sensing process, so less dependence on sample flow rate or stirring speed; no requirement for electrodes or electrolyte; ultra-low cost of probe head, combined with convenient multi-point polling via optical fibre switches; immunity to high external pressure; fibre probe connection allowing monitoring in remote, hazardous or in vivo applications; no influence of Ca^{2+} and Mg^{2+} (unlike micro-electro-chemical sensors). Finally, as they have no electrolyte, the sensors can function in micro-gravity (spacecraft) conditions.

Optical oxygen sensors are slowly gaining market share with respect to their electro-chemical counterparts. One of the first commercially available oxygen sensors was the FOXY (Fiber Optic Oxygen Sensor)[8], which has been available since 1998. In this system, a sensing membrane at the probe tip gives the oxygen readings in conjunction with blue LED excitation and a CCD spectrometer. When a large operating temperature range is required, additional temperature compensation is necessary, and this is achieved by use of electrical leads to a thermocouple in the sensing head, taking away a basic advantage of the probe, its non-electrical nature. A competing commercial oxygen sensing system[9] measures probe temperature with a resistive temperature sensor. We will describe our new all-optical temperature compensation system, which has advantages over electrical systems.

Another commercially available oxygen sensor[10] operates by interrogation of the fluorescence decay response from the indicator dye, using a 'boxcar' (single temporally-scanned time-slot over the period of the fluorescence decay) signal averaging scheme.

New applications and areas for optical oxygen sensing are emerging all the time. Two examples are (a) sensors designed with fast response for real-time respiration measurement [9] and (b) multi-channel oxygen-imaging systems [7] for measuring the variations of oxygen concentration in human skin tissue.

Though much published work describes the synthesis and characterisation of Ru^{2+}-based indicators in the literature, few publications pay detailed attention to designing efficient interrogation systems to monitor the indicators. The more detailed work presented here is focused toward enhancing the precision, speed of measurement, and reliable calibration of such sensors.

Basic methods of Fluorescence Monitoring for Oxygen Sensors

Oxygen is an effective dynamic quencher of many types of fluorescence and phosphorescence. In fact, the presence of oxygen in air is often considered a hindrance to chemists when attempting to accurately measure luminescence lifetimes and quantum yields of their test species. This can, however, be constructively used to sense gaseous or dissolved oxygen levels by monitoring the fluorescence response from a suitable indicator dye. Ru-based indicator dyes, when encapsulated in silicone or sol-gel matrices, are commonly chosen for their strong and long-lived fluorescence (500ns – 12μs), their large measurement dynamic range, fast response time, large Stokes shift, and strong blue/green absorption.

Though fluorescent indicators could be interrogated simply by applying a constant excitation intensity and monitoring changes in the ***intensity*** of the resultant fluorescence, this usually leads to stability and calibration problems, and is therefore undesirable. Degradation or leaching of the dye from its support matrix, changes in excitation power, or changes in leads couplers or connectors can all cause unwanted changes in the returning fluorescent intensity. In particular, undesirable variations in the plug-in probes themselves, e.g., due to connector terminations, geometrical alignment factors or variations in dye concentration at the sensing tip will necessitate individual calibration of every probe, with possible variations when taken off and reconnected, or if leaching or photo-bleaching of dye occurs.

These problems are avoided by interrogating the fluorescent decay of light from the membranes in the time-domain, so that measurements are made independently of fluorescence intensity. The light source could be an intensity modulated laser, LED or flashlamp and the fluorescence decay lifetime can effectively be determined from the temporal decay of the re-emitted fluorescence light. Most modern interrogation systems for Ru-based indicators monitor fluorescence lifetime, as the decay time constant (usually >500ns) or parameters related to it, may be easily measured with simple electronics.

Lifetime Sensing Schemes

There are two well-known approaches for interrogating the fluorescence lifetime of chemical probes. Most practical chemical sensors have measured the fluorescent lifetime by monitoring the phase delay between the modulated incident light from a blue LED and, by means of a photodiode, the detected (orange-red) fluorescence signal returning from the dye[11,12]. Alternatively, interrogators employing photon-counting detection have been described, coupled to either time-gated electronic counters[13] or multi-channel acquisition systems (as used in [14], [15]). Photon-counting sensors offer advantages over phase-based sensors in certain applications, particularly when the so-called "Rapid Lifetime Detection" (RLD) algorithm is used. Until recently, the large size, cost and complexity traditionally associated with photon-counting has prevented practical use of these in low-cost portable instrumentation.

Research At Southampton

This paper describes the ongoing research at Southampton University to enhance Ru^{2+}-indicator-based oxygen sensors.

Firstly, our custom-designed and built phase-delay and photon counting interrogation systems are described. Though the principles used have been described elsewhere[16 17], our instrumentation[18] contains some novel features to enable versatile sensor testing and calibration.

Secondly new results from recently developed mathematical models of the Rapid Lifetime Detection photon-counting sensor are discussed, and their relevance to the optimization of the sensing algorithm is shown. An analytical approach to modeling all the parameters has, to our knowledge, never been explored before. Using our model, sensors may either be optimized for operation with one set of static pre-defined parameters (where the calculations would be applied once only at design time, based on expected signal and background light levels) or, when higher precision or wider dynamic range of measurement is required, it could allow re-calculation of sets of chosen parameters during operation, depending, for example, on the oxygen concentration point or on the level of received light for the desired range of operation. Note, however, that for general-purpose instruments, designing too much sophistication into the system would lead to high costs and complexity.

Thirdly, our novel probe, allowing simultaneous temperature and oxygen measurement is described. The probe provides optical on-line thermal monitoring of the sensor. Both temperature and oxygen may be interrogated with either phase-delay or photon-counting detection schemes. No extra optics, and only simple additional electronics is required in the sensor instrumentation to enable the probe to perform the additional temperature measurements.

Finally, by combining the mathematical model with our previously reported calibration probe, we suggest a new calibration and sensor testing procedure. Results from the procedure can be used not only to calibrate sensors, but also to diagnose interrogation malfunctions arising from undesirable factors such as background fluorescence from other sources (fibers, lenses and contaminants), detector overload and any variations in the interrogator response.

OPTICAL ARRANGEMENTS TO ADDRESS OUR FIBRE PROBE

Most Ru^{2+}-based oxygen indicators absorb blue light strongly, returning Stokes-shifted (red) fluorescence. Laser, LED or flash-lamp sources have been used to excite the indicators, but for most practical sensor applications, the high-brightness blue LED is preferable. Photodiode, APD or PMT detectors can measure the returning fluorescence light. To provide the necessary wavelength-selective coupling between excitation LED, fluorescent dye and detector, an optical coupling assembly is required.

Several optical arrangements for interrogation of Ru^{2+}-based layers have been reported. In our own system, to provide efficient wavelength-selective directional coupling between excitation LED, fluorescent dye, and detector, an optical filter block, employing a 45° dichroic filter has been designed and custom built. This allows excitation and interrogation of the desired indicator layers with a single optical fibre.

The indicator layer is excited with intensity modulated radiation in a narrow range of wavelengths centered around 470nm, with a peak power of 410nW. This is derived from an ultra-bright blue LED (HP type HLMP-CB15) passing through a shortpass (blue-transmitting, red-blocking) filter, set to remove residual long wavelength radiation. This light is then coupled to the fibre via a 45° dichroic filter, configured as a beam splitter, which preferentially reflects the blue excitation light wavelength. The returning fluorescence is then collected by the same fiber. The red fluorescence signal is now transmitted by the 45° dichroic beam-splitter to impinge, via a final long-pass (red transmitting, blue-blocking) filter set, onto a detector. Figure 1 is a schematic layout of the optical filter block.

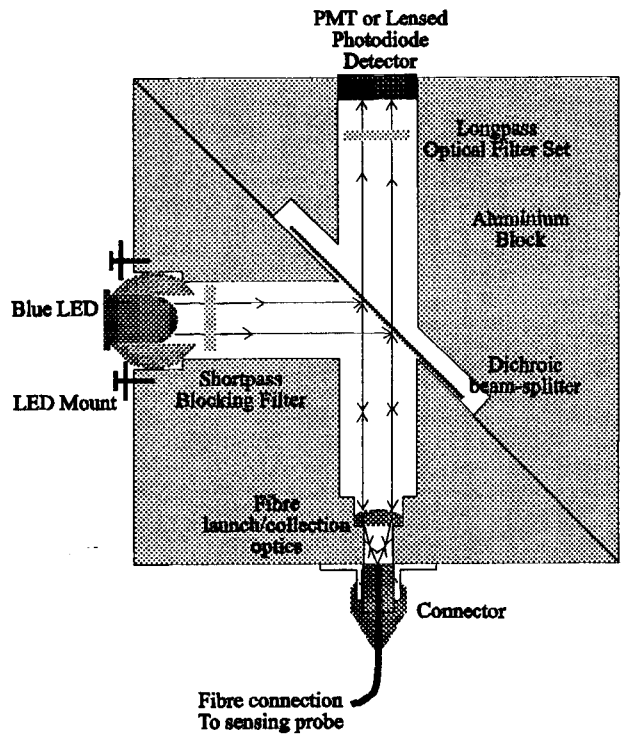

Figure 1 Dichroic optical coupling system to launch LED light into, and collect fluorescent light from, a fibre probe (near-end of probe cable is mounted in an FC connector in the FC mounting plate at the bottom of the figure)

As there is a large wavelength shift between the (blue) absorption peak and the (orange-red) emission peak of an Ru^{2+} indicator, the optical design requirements for a fluorescence interrogation system are relatively straightforward. However, special attention must always be given to sources of unwanted fluorescence.

It is extremely undesirable to have other fluorescent materials in the optical path, as some of their fluorescence light could return to the detector, and be confused with desired signals from the chemical sensing membrane. Unwanted fluorescence decay signals at the detector provide, at best, an offset to measured fluorescence decay lifetimes, and at worst, a temperature dependent offset that causes an unpredictable error. LEDs, absorbance type (coloured-glass) optical filters, certain common types of optical cements, oil films, connectorised optical fibre leads, and even fingerprints have been found to fluoresce red when exposed to blue excitation light.

One particularly important source of unwanted fluorescence was found to arise from the standard epoxy used by optical fibre connectorised lead manufacturers to secure the fibre into its connector ferrule. Stray excitation light, falling on the exposed adhesive at the fibre tip, can excite the epoxy and cause a large fluorescence light signal. To alleviate this, a non-fluorescent cement suitable for bonding the fibre into its ferule should be used. For our system, a styrene glue (designed for

clear casting applications) was chosen for its very low absorption and fluorescence re-emission characteristics and our own leads were custom constructed.

PHASE-SENSITIVE DECAY TIME MEASUREMENT

Phase delay detection techniques are commonly used for Ru^{2+}-layer interrogation because of the low cost of optical and electronic components required, simplicity of the detector, and reasonable tolerance to background light.

In these systems, the drive current to the LED is modulated (usually sinusoidally) at a frequency f_m. The returning weak fluorescence from the indicator layer is also modulated at frequency f_m, but returns with a total delay arising from a combination of electronics delays, optical propagation delays, and a variable delay, which is a function of the fluorescence lifetime. The value of the latter is derived as our indication of the state of the indicator. In the case where the LED is modulated with a sine wave, the indicator lifetime, τ, and the phase delay, ϕ, are related by

$$\phi = -\tan^{-1}(2\pi f_m \tau) \quad (1)$$

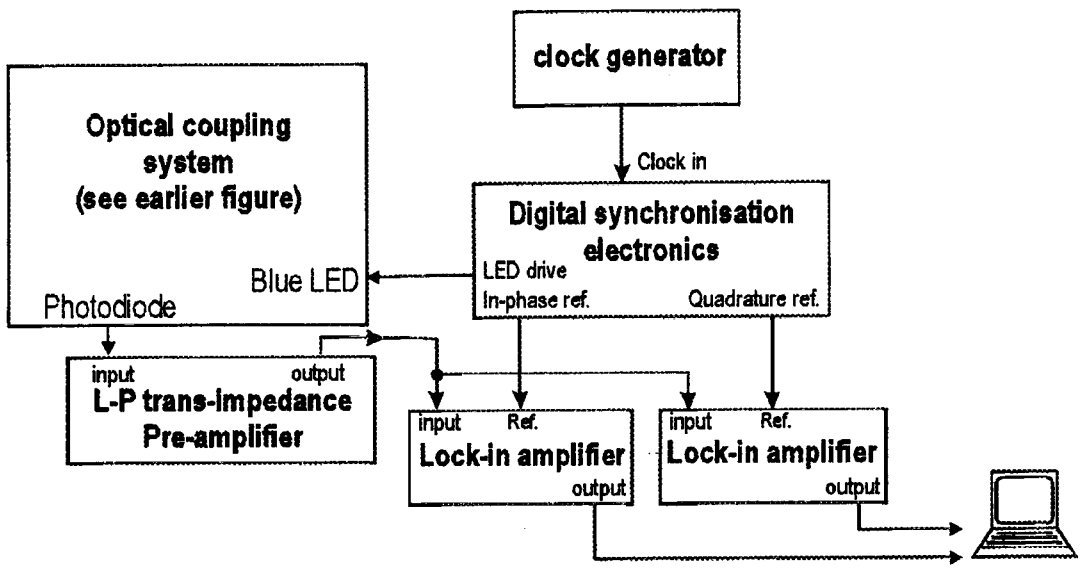

Figure 2 A schematic diagram showing the electronic elements in our phase-based fluorescence lifetime sensor for Ru-based oxygen sensor indicator interrogation

In our system, the LED is square-wave modulated to simplify the electronics. The LED drive signal, and digital synchronisation signals are produced by division of a pre-settable master clock, allowing computer selection of the master operating frequency. A TTL square wave, (termed D_0) and one delayed by 90 degrees to it, (D_{90}) are passed as reference inputs to a pair of electronic multiplier circuits (lock-in amplifiers), each followed by low-pass filters to decode both in-phase and quadrature components of the detected signal. The LED modulation signal may be delayed relative to the D_0 and D_{90} signals, allowing optimum biasing of the phase delay in the lock-in arrangement to ensure lowest measurement error. The in-phase and quadrature outputs (two DC signals, V_0 and V_{90}), are applied to a control PC via analogue interface.

Optimum calibration of such phase sensors for oxygen measurement, and identification of the most favourable modulation frequency have been considered before[19], so we will not enlarge on this here.

PHOTON-COUNTING DECAY-TIME MEASUREMENT

Photon-counting lifetime sensor systems, based on either timed gating of electronic counters or multi-channel acquisition, are an alternative to phase-delay measurement schemes.

Photomultiplier tubes are commonly used for photon counting detection. When a photon strikes the photocathode, there is a finite probability that a photoelectron will be emitted. These electrons are then multiplied by a cascading action at each of a subsequent series of charged dynodes and detected at the anode. At high light levels, the photoelectrons resulting from each detected incident photon overlap, producing an analogue voltage at the anode that is proportional to the received light

intensity. At low incident light levels (<~10 M photons s^{-1}), the electrons arriving at the anode arising from each detected photon can be separated, detected via an electronic discriminator circuit, then shaped into convenient digital pulses ready for subsequent digital processing. The photon count per second is then related to the light intensity in a highly linear manner until pulse coincidence becomes significant. In the case of a fluorescence interrogation system (where the received light level is usually low), the total photon count frequency observed is the addition of photoelectrons arising from detected (fluorescence) photons, plus a background resulting from ambient background light, and finally an unavoidable (though cooling can reduce it) contribution (the so-called 'dark count') arising mainly from thermally induced electrons produced at the anode or dynodes. Poisson counting statistics dictates that the intrinsic error in a measurement of n randomly-arriving photons is $\sqrt{n}$.

Photon counting detectors in fluorescence lifetime interrogators can lead to several advantages in comparison to diode detection under certain conditions.

Firstly, by counting individual photons, it is possible to work at light levels below the detection limit of a photodiode-based system. This permits interrogation of dyes having poor photo-bleaching behavior and/or very low quantum efficiencies. As less returned fluorescent light is required, they may more easily be addressed via single fibres instead of thick fibre bundles.

Secondly, due to the time gated detection used, a photon counting system may more easily separate excitation light from fluorescence. In conventional fluorescence measurement systems, some cross-talk light, albeit significantly attenuated by a well-designed filtering system, will inevitably appear at the detector and change the apparent phase of the returning fluorescence. This can occur due to imperfect filters or due to fluorescence in adhesives, etc, which generally have very much shorter decay time. Because it only measures signals after the excitation light pulse, a photon counting interrogator is intrinsically immune to such cross-talk, as the elastic scattering signal and the short-decay fluorescence signals disappear as soon as the light source is extinguished.

Thirdly, a photon counting system can more easily be configured to monitor the actual fluorescence decay curve of materials, (multi-channel systems already immediately recover decay curves, and time gated systems display curves by setting the control algorithm to build up a curve by sequential "boxcar" detection). A band-limited phase detector system cannot follow time decay curves and a high bandwidth system would be noisy.

The disadvantages of the photon-counting approach, when compared with phase delay systems are: the expense of the detector (though PMTs are recently becoming cheaper), and their sensitivity to background light. Conversely, a photo-diode detector and pre-amplifier is inexpensive, and as long as the electronics is not overloaded, the frequency selective lock-in amplifier used is not susceptible to incoherent background ambient light.

Until recently, though often used in laboratory bench-top experiments, fluorescence measurement instrumentation employing photon counting detection schemes have not been widely pursued, due to the additional expense and bulk of the detector, and the need for sophisticated real-time curve-fitting. Recently, new compact and low-cost, modular photon counting heads, complete with integral DC/DC converter, pulse height discriminator, pulse shaping electronics (e.g. Hamamatsu type H6180 and new red-sensitive modified versions) provide versatile photon-counting detection. When the interrogator operates using the RLD sensing scheme, which requires simpler hardware and software than maximum likelyhood or least-squares- curve fitting algorithms, a highly attractive alternative to the phase-based sensor is achieved.

The Rapid Lifetime Detection method (RLD)

The so called "Rapid Lifetime Detection (RLD)" method[20 21 22 23] is a fluorescence interrogation technique based on accumulation of all the fluorescence-light-induced PMT anode pulses arriving within two or more time intervals. It allows extremely rapid evaluation of fluorescence intensity and lifetime, with modest interrogation hardware, yet can be almost as accurate as the more sophisticated maximum likelihood estimation technique[24], which requires multi-channel acquisition of the fluorescence decay curve. Here the basis of the RLD technique is briefly discussed, then some of the results from our new modeling and parameter optimization work based on this method are reported.

It is important to note that RLD techniques, and the optimisation results calculated in this work can be applied to CCD based fluorescence lifetime imaging systems for detecting extended lifetimes, as the charge accumulation and collection principle of CCDs is equivalent to the time-gated photon counting sensing scheme discussed here.

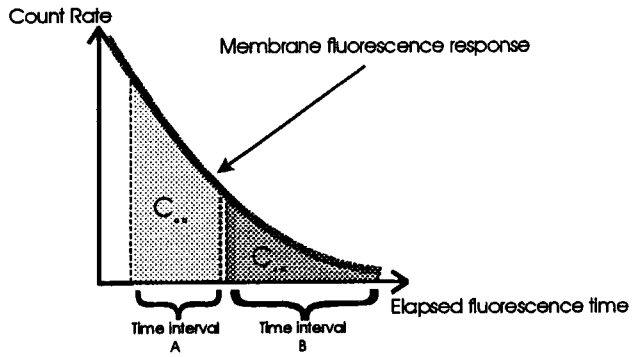

In Figure 3, the fluorescence light decay is plotted, in terms of the detected photon arrival rate (~ intensity) as a function of time after excitation by a short pulse of blue light. In the RLD technique, simple digital electronics is used to count the number of anode pulses arriving in two pre-defined time intervals (time windows). The two accumulated values, C_{ab} from the detected photons arriving in time interval A, and C_{cd} from those arriving in time interval B, are passed to a control computer (see Figure 4).

Figure 3 The RLD sensing scheme. The ratio (C_{ab}/C_{cd}) of photons counted in time intervals (or windows) A and B is processed to derive the measured value

In traditional RLD, two ***equal duration*** sequential time-windows are used to interrogate the decay, and (for mono-exponential fluorescent decays only) the lifetime can be derived from C_{ab} and C_{cd} via simple equations. The arrangement of electronic elements within our fluorescence lifetime measurement system is shown in Figure 4. The unit operates using an enhanced RLD technique. Our synchronization hardware incorporates a RAM lookup table, allowing flexible computer controlled allocation of window intervals, excitation pulse duration and overall repetition rate. Wide variation in averaging time is also possible.

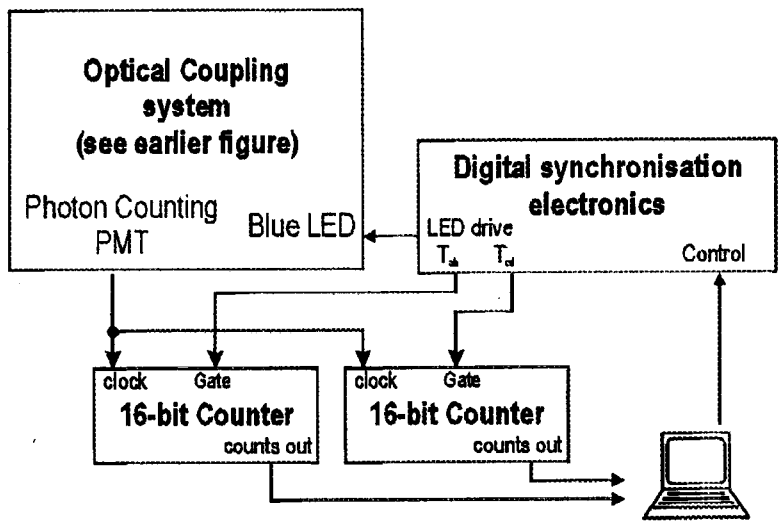

Figure 4 Schematic arrangement of our photon-counting fluorescence interrogator designed for use with the Rapid Lifetime Detection algorithm. Our synchronization hardware incorporates a RAM lookup table, allowing flexible computer controlled allocation of window intervals, excitation pulse duration and overall repetition rate. Wide variation in averaging time is also possible.

Various schemes have been suggested for enhancing the traditional RLD sensor for greater precision, ability to withstand background light, and interrogation of multi-fluorescence decays by introducing overlapping and multiple time windows. In our research, we have considered all of the following:- the possibility of time windows of any start time and duration, varying excitation pulse width, compensation for constant background and dark light intensity and residual fluorescence from previous decays (this is important in high-repetition rate applications and this varies as the indicator lifetime changes).

Theory of sensing system

We intend that our detailed theoretical study of the RLD technique and optimization of RLD sensors will form the basis of a submission for another extended journal publication, so here we present only a short summary of some results from this work. The aim of the model is to identify optimum window boundary, repetition rate, and excitation pulse length conditions that lead to maximum precision measurement.

Mono-Exponential, Background-less model

We shall initially consider an indicator with an ideal mono-exponential fluorescent decay, operating in zero background light and assume no dark count from the PMT. It is assumed that our aim is to measure the exponential decay lifetime with maximum Signal to Noise Ratio (SNR) in the presence of photon-counting noise obeying Poisson counting statistics.

It can be shown that, when a single excitation pulse (beginning at time t=0, and ceasing at $t=t_{off}$), falls on an indicator, having a mono-exponential fluorescent decay of lifetime τ, the fluorescence intensity observed after time t_{off} is,

$$I_1(t) = \left[\tau I_s.(1-e^{t_{off}/\tau})\right].e^{-(t-t_{off})/\tau} \qquad (2)$$

Using the above formula, Figure 5 shows the expected response from a lifetime sensor, using an indicator with 3μs decay. This is taken after excitation using incident pulses of 3 different durations 5,10 and 30μs. An increase in excitation pulse duration does not yield a proportionate increase in the received post-excitation fluorescence intensity, because the peak fluorescence intensity approaches an equilibrium value, where the number of fluorescent sites excited per unit time equals the number of these relaxing to a lower state. However, increasing the excitation pulse width has the undesirable effect of decreasing the possible repetition rate, which tends to reduce the achieved measurement precision. There therefore exists an optimal excitation pulse duration, where the best trade-off between fluorescence intensity and repetition rate is achieved.

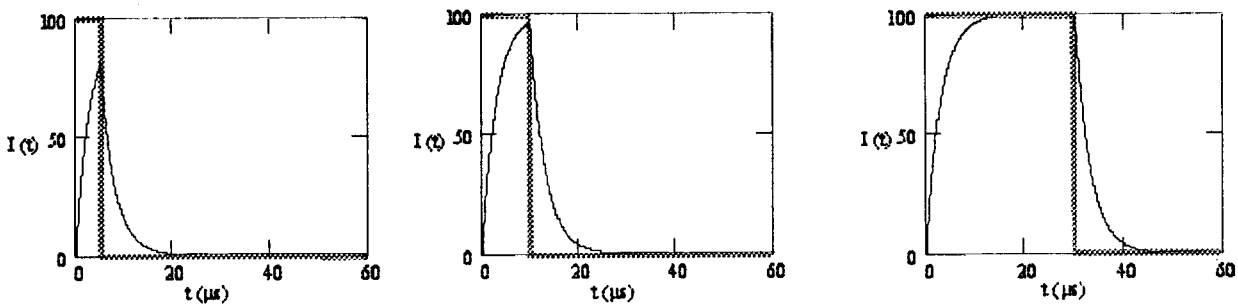

Figure 5 Theoretically observed fluorescence decay profiles from a sensor probe with 3μs mono-exponential decay. These are taken during and after exposure to several different duration (5, 10, 30 μs) single excitation pulses. Note that increasing the duration of excitation pulses does not yield proportionaly larger post-excitation fluorescence intensities.

Our model was extended to account for the weak, but finite, residual fluorescent "tail" from previous excitation pulses and the Signal to Noise Ratio (SNR) in measurement of τ was calculated analytically by noise propagation arguments (we assumed that for strongly-fluorescing Ru^{2+} indicators, noise components can be thought of as representing small perturbations to the overall signal). The calculated SNR was scaled to account for the experimental repetition rate, and this time-normalised SNR was maximized (using Powell's multi-dimensional algorithm[25]) in terms of the 6 dimensional setup vector (t_1,t_2,t_3,t_4,t_{off},t_{rep}), where t_1 and t_2 are the start and end times for time interval A, t_3 and t_4 are for time interval B, t_{off} is illumination flash duration and t_{rep} is the overall experiment repetition period.

For test purposes, an instrument designed to measure the fluorescence decay time of a mono-exponential sensor of lifetime 3μs and I_s of 100 counts.s^{-1} was considered, giving the optimum condition presented in Figure 6.

Parameter	*Value (μs)*
t_{off}	6.057
t_1	6.057
t_2	7.793
t_3	11.218
t_4	19.769
t_{rep}	19.769

SNR = 2.767 $Hz^{-0.5}$ (single repetition)

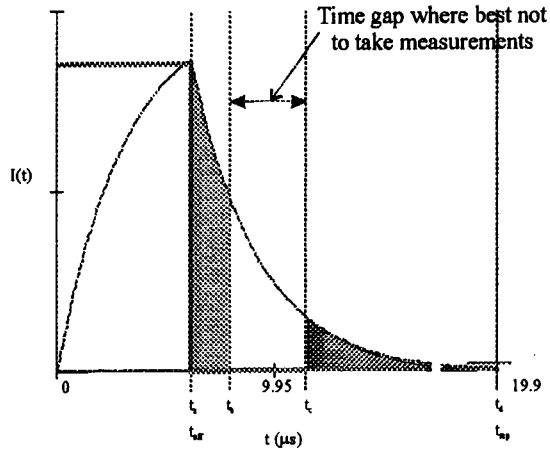

Figure 6 Schematic illustration of the optimum configuration of setup parameters for the determination of a 3μs fluorescence decay lifetime using a two time window RLD method in the absence of background ambient light. Note the time gap where, surprisingly, it is advantageous not to measure any light in order to minimise the error in the lifetime determination

Figure 6 shows that, at the most favourable measurement condition, there exits a short time gap between the first and second windows, during which no counts are accumulated. Thus, it is actually advantageous to ***not*** use some of the available photon counts.

Next, a sensor designed to measure the varying 1-10μs lifetime of a mono-fluorescent indicator with maximum SNR was considered. For each expected lifetime value, there exits a new optimum setup vector. Figure 7 plots the optimum time window boundaries for maximum SNR determination of decay lifetime as a function of sensor decay lifetime. The optimum SNR is also plotted (using the axis on the right). We see to maintain the optimum lifetime determination over a 1 to 10μs decay time range requires large changes in the setup parameters.

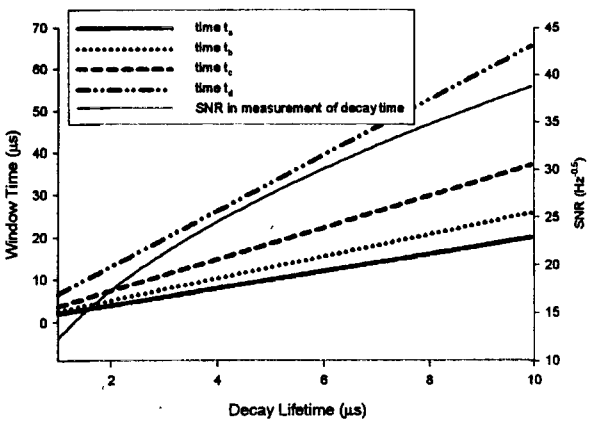

Figure 7 Theoretical values of the optimum time window boundaries, plotted as a function of a fluorescence decay lifetime. The value of optimum SNR for determination of decay time is also plotted.

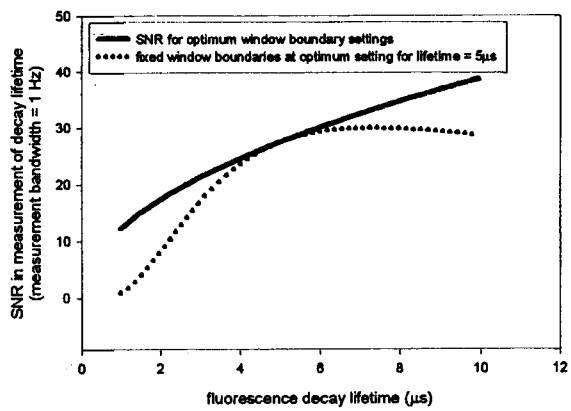

Figure 8 Comparison of the optimum SNR achievable when using a variable optimisation routine to the SNR achievable using a fixed setup vector

We shall now illustrate the SNR penalty if we were to take measurements with only a single setup vector over the entire measurement range. Figure 8 shows a comparison of the optimum SNR attainable if we were to ***vary*** the setup vector to suit the prevailing decay lifetime (from Figure 7), with the non-optimum SNR attained when the setup vector is **fixed** at one initially selected value (corresponding to the optimum for measurement of 5μs fluorescence decay lifetime). For shorter lifetimes, the SNR achievable from fixed parameter measurement quickly approaches zero. For this sensor, a selection of setup parameters, based on a preliminary measurement of the then lifetime (perhaps via an auto-ranging algorithm) would be necessary for low-noise operation over the entire measurement range.

Mono-Exponential, Constant background model

Our model described so far has been incomplete, as we have neglected the effect of background ambient light on the readings. In reality, a small amount of unwanted constant background is inevitable. This can arise from ambient light, and partly from the unavoidable 'dark count' in the detection system. By including a "background" term in the model, the effect of dark counts and background-light counts on the SNR in determination of τ has also been determined. We considered a very high light level sensing element (to reduce irrelevant statistical errors and cut computation time), returning a mono-exponential decay of lifetime $\tau = 3\mu s$, and intensity term $I_s = 100(\text{counts}/\mu s)$. Figure 9 shows (solid curve) the maximum attainable SNR in determination of τ, after 1s of averaging, plotted as a function of background light level in counts/μs (N_d). Background levels of between 0% (N_d=0) and 10% (N_d=30) of the peak response to a delta-function excitation pulse were considered. The dotted line shows the SNR achieved when the setup parameters are fixed at their background-less optimum values. The optimum measurement situation, achieved by optimizing setup parameters to suit the prevailing background level, leads to significantly superior SNR.

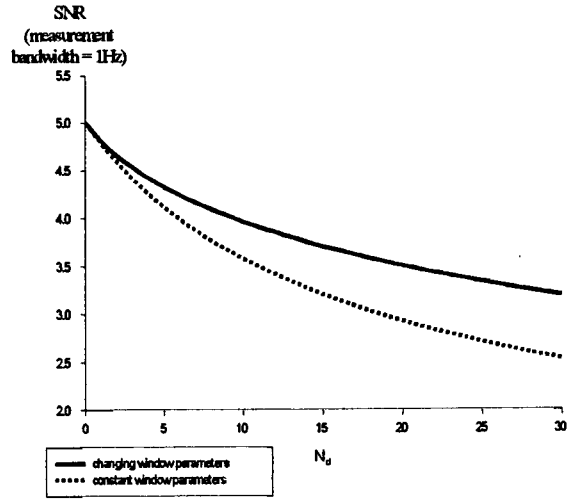

Figure 9 The effect of background light on the optimum SNR for the determination of lifetime (i.e. that with a variable setup vector routine) (in black) plotted against SNR possible with fixed window boundary parameters (in red).

The analytically derived model was verified by comparison with both a computer simulated RLD sensor, and a real laboratory RLD interrogator. The test decay profile for all three situations was mono-exponential, with 3μs lifetime. Firstly, expected values for count ratio (r), and SNR in r were calculated at each of 130 chosen setup vectors (including the expected optimum vector) using the analytically-derived error-propagation model described above. A computer simulated RLD sensor, (based on adding Poisson photon-arrival statistics to the theoretical decay curve), was programmed to simulate values for r and SNR in r at each setup vector, and the results compared with the previously calculated (expected) values. A laboratory RLD interrogator was connected via optical fibre to a test sample of Ti:Sapphire crystal (which returns mono-exponential fluorescence decays). The crystal was thermally controlled to return 3μs fluorescent lifetime while the interrogator was set to take measurements at each of the 130 setup vectors. The measured count ratio, r, and the achieved signal to noise ratio in the measurement of r were logged. All three sets of results show excellent quantative agreement, proving (at least for the chosen fluorescence light intensity and actual background level) the validity of our analytical error-propagation model.

Double-Exponential, Constant Background model

In reality, most encapsulated fluorescence indicators used for chemical sensing do not return pure mono-exponential decays, due to the heterogenous nature of the support matrix (see e.g.[26]). Many models to explain the observed decay profile have been suggested, but perhaps the most popular is the 'two-site model'. When encapsulated in a support matrix, the indicator molecules are bonded to spectroscopically heterogeneous sites, with the Stern-Volmer equation holding for each site. In the two-site model, it is assumed that only two types of site exist within the membrane, leading to a double-exponential fluorescence decay curve. Our model has recently been extended to incorporate the two-site model, and optimum conditions for sensing oxygen levels have been computed, and we are currently experimentally verifying these results and hope to report later.

COMBINED TEMPERATURE AND OXYGEN PROBE

One of the known problems with Ru^{2+} based oxygen sensors is that their sensitivity varies significantly with temperature. This dependence occurs with most fluorescent-lifetime-based chemical probes, as the occupancy and hence the decay rates of electronic levels vary considerably with temperature. It is therefore desirable to mount a temperature sensor at the probe tip to monitor and correct for thermal changes. Clearly, a simple thermocouple could be used, but this requires a separate

interrogator and throws away one of the major attractions of the probe, its non-electrical nature. We decided it is preferable to use an optical temperature probe that can be interrogated via the same optical lead as the chemical sensor, and use the same opto-electronic interrogation system as for the chemical measurand, giving an almost ideal solution.

We have previously reported[27] our optical temperature compensation system, which uses a small ruby crystal insert to measure temperature and allow compensation for the thermal dependence of the Ru^{2+} chemical sensor. The same optics is used to excite and collect light from both the Ru^{2+} and the ruby crystal. An earlier optical temperature compensation system[28] used an alexandrite crystal to monitor the temperature of a platinum tetraphenylporphyrin (PTPP) indicator, and the interrogation system measured the electronic frequency spectrum of the detected fluorescent signal. Although this worked in practice, it required a complicated high-frequency signal processing scheme, which can give inferior signal/noise ratio when compared with low frequency electronics. Also, our combination of ruby crystal and Ru^{2+}-layer has a far greater ratio of crystal to layer fluorescent lifetime than the earlier alexandrite/ PTPP combination, and ruby, unlike alexandrite, is non toxic.

In our case, the detailed fluorescence light from the ruby crystal is readily separated from that from the chemical sensor because of the crystal's much longer fluorescence lifetime. The ruby crystal has a lifetime (Figure 10) approximately one thousand times longer than that of the chemical sensor layer, so both lifetimes can be easily measured, simply by changing the system clock rate.

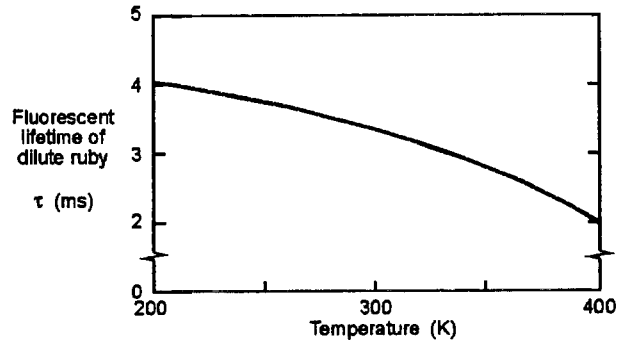

Figure 10 Fluorescent lifetime of ruby crystal plotted as a function of temperature. Note, around room temperature, the fluorescence lifetime (~3ms) is over one thousand times longer than the Ru^{2+} dye lifetime (~3-5μs) D.F. Nelson and M.D. Sturge, Phys. Rev. 137 A1117 (1965)

Several optical arrangements are possible for the combined ruby and membrane probe, all based on a single (600μm core, 660μm cladding) fibre for excitation and collection. The most successful design so far has been to simply bond a thin layer of ruby crystal to the polished fibre end with the chemical sensing membrane then bonded to the ruby disc. Excitation light emerging from the fibre passes through the disc, exciting the ruby crystal, and the remaining light falls on the membrane. Fluorescence from both the membrane and the ruby is partially coupled back into the fibre.

RU SENSOR CALIBRATION

To avoid errors, (e.g. during industrial quality assurance) there is a need to calibrate the interrogation system, using a standard plug-in probe. This should allow checking of the interrogator independently of the external chemical sensing probe, as the latter could have its own variability due to changes in composition, support matrix, and of course oxygen level. Once this interrogator calibration has been performed, the chemical sensing probe may be either factory calibrated independently, or by using the validated interrogator itself.

We have previously reported a thermally controlled Ti^{3+}-doped-sapphire crystal fluorescence lifetime calibration standard[29], [30], using a small cuboid (2.0x1.5x5mm) of Ti^{3+}- sapphire, bonded on the distal end of the fibre probe. This calibration probe is thermally controlled with a Peltier heat pump. The fluorescence lifetime of this type of calibrator is stable with time, even under intense excitation. The optical stability has been proven in many years of Ti:sapphire laser use, is insensitive to chemical species, and may be predictably tuned simply by varying its temperature.

We now suggest a new verification and testing procedure for interrogators for RLD photon counting fluorescence (described above), which has been inspired by the experiment to verify our analytical model for mono-exponential decays. The procedure for calibration is as follows. At the desired test lifetime, expected values for count ratio (r) would be calculated at each of a number of chosen setup vectors (i.e. interrogator setup parameters), using the analytically derived error-propagation model for mono-exponential decays described above. An RLD interrogation system under test would then be

connected to the plug-in calibration probe, and the temperature control set so that the calibrator returns the desired test fluorescence lifetime. The interrogator would then be programmed to measure count ratio (r) at each of the chosen setup vectors. Any disagreements between expected and measured count ratio would indicate an error in the interrogation system. The error might arise from unwanted fluorescence, optical or electronic delay, or perhaps malfunction. Interrogation problems could be diagnosed by identifying which parameter combinations lead to errors. A comparison graph plotting measured count ratio and exponential theoretical count ratio is shown in Figure 11, where our RLD interrogator was tested over 130 setup conditions at a 3μs decay lifetime. The excellent quantative agreement confirms a healthy operation of our interrogation system.

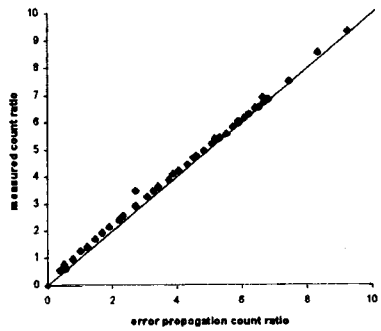

Figure 11 Comparison between the measured count ratio and the theoretical count ratio from the analytical noise propagation of a mono-exponential decay. A 130 member set of setup vectors (i.e. window boundary times and repetition rate) was chosen and the expected count ratio for each vector calculated using the analytical mono-exponential model (described above). The experimental interrogator was operated at each setup vector, and the resultant count ratio logged. The figure shows both ratios plotted together. The excellent agreement reflects calibrated operation of the interrogator.

CONCLUSION

In this paper we have described the present state of continuing research at Southampton to enhance the interrogation, temperature stability and calibration of Ru-based optical oxygen sensors. Brief results and description of a new analytical model of our Rapid Lifetime Detection interrogator are presented. The model has been used to identify optimum setup conditions for such interrogators and was checked against experiment. The model, which can be easily applied to CCD based imaging systems, will hopefully be described in more detail in a forthcoming technical paper. The model is used in conjunction with our previously reported Ti^{3+} - doped sapphire fluorescence-lifetime calibration probe to provide a new interrogator testing and verification procedure.

ACKNOWEDGEMENTS

Part of this work was performed under an EC Brite-EURAM IV programme (contract no. BRPR-CT97-0485, Biocompatible Optical Sensor Systems, called "BOSS"). The authors thank Prof. G. Orellana (Universidad Complutense de Madrid) for providing the Ru^{2+}-based silicone impregnated layers used in this work.

---

[1] H. Schmidt H. Kronfeldt, "Submersible Fiber-Optic Sensor System for Coastal Monitoring", Sea Tech., 51-55,1999

[2] M. Lee, et. al., "Visualization of oxygen concentration in water bodies using a fluorescence technique", Wat. Res., **34**, 2842-2845,2000

[3] B. Grunwald G. Holst, I. Klimant, M. Kuhl, A luminescence Lifetime Imaging System Using Imaging Fibers to Measure the 2D Distribution of O2 in Biological Samples, *SPIE Fiber Optic Sensor Technology and Application*, 3860, SPIE, 1999

[4] C. Kolle, et. al. C. Kolle, "Fast Optochemical sensor for continuous monitoring of oxygen in breath-gas analysis", Sens. Actua. B, **38**, 141-149,1997

[5] F. Baldini, et. al. F. Baldini, Optical Fibre Chemical Sensors at IROE for Medical Applications, *Biochem. Med. Sens.*, 2085, SPIE, 1993

[6] Yet. al. Y. Gu, "A new fiber optic sensor for detecting in situ the concentrations of pharmaceuticals in blood", Sens. Actua. B, **66**, 197-199,2000

[7] L. Schulze M. Stucker, G. Pott, P. Hartmann, D. Lubbers, A. Rochling, P. Altmeyer, "FLIM of luminescent oxygen sensors: clinical application and results", Ibid., **51**, 171-175,1998

[8] Ocean Optics, "FOXY Fiber Optic Oxygen Sensor", 1996

[9] photosense LLC, "Photosense www.photosence.com/oos.html", currently in R&D phase

[10] Van Essen Instruments, "O2 sensor for ground and surface water monitoring", R&D phase

[11] D. Ackley M. Murtagh, M. Shahriari, "Development of a Highly Sensitive Fibre-Optic O2/DO sensor based on a phase modulation technique", Elec. Lett., **32**, 477-479,1996

[12] C. Kolle W.Trettnak, F. Reininger, C. Dolezal, P. O'Leary, "Miniaturized luminscence lifetime-based oxygen sensor instrumentation utilizing a phase modulation technique", Sen. Actua. B., **35**, 506-512,1996

[13] Van Essen Instruments, "O2 sensor for ground and surface water monitoring", R&D phase

[14] D. Birch G. Hungerford, "Single-Photon timing detectors for fluorescence lifetime spectroscopy", Meas. Sci. Technol., 7, 121-135,1996

[15] P. Selvin M. Xiao, "An improved instrument for measuring time-resolved lanthanide emission and resonance energy transfer", Rev. Sci. Instr., **70**, 3877-3881,1999

[16] C. Kolle W.Trettnak, F. Reininger, C. Dolezal, P. O'Leary, "Miniaturized luminscence lifetime-based oxygen sensor instrumentation utilizing a phase modulation technique", Sen. Actua. B., **35**, 506-512,1996

[17] D. Ackley M. Murtagh, M. Shahriari, "Development of a Highly Sensitive Fibre-Optic O2/DO sensor based on a phase modulation technique", Elec. Lett., **32**, 477-479,1996

[18] E. Austin and J. Dakin, Recent measurements with Ru2+ oxygen sensors, using doped sapphire crystals, both as a calibration aid and an integral temperature sensor (invited paper), *Fiber Optic Sensor Technology II*, 4204, SPIE, 2000

[19] D. Papkovsky V. Ogurtsov, "Selection of Modulation Frequency of Excitation for Luminescence Lifetime-based Oxygen Sensors", Sen. Actua. B.,'**51**, 377-381,1998

[20] C. Wilkerson Jr J. Tellinghuissen, "Bias and Precision in the estimation of exponential of Exponential Decay Parameters from Sparse Data", Anal. Chem., **65**, 1240-1246,1993

[21] A. Periasamy K. Sharman, H. Ashworth, J. Demas, N. Snow, "Error Analysis of the Rapid Lifetime Determination Method for Double-Exponential Decays and New Windowing Schemes", Ibid., **71**, 947-952,1999

[22] D Burns P Waters, "Optimized gated detection for lifetime measurement over a wide range of single exponential decays", App. Spectro., **47**, 111-115,1993

[23] J Demas R Ballew, "Error analysis of the rapid lifetime determination method for single exponential decays with a non-zero baseline", Anal. Chem. Acta, **245**, 121-127,1990

[24] B. Legendre Jr. S. Soper, "Error Analysis of Simple Algorithms for Determining Fluorescence Lifetimes in Ultradilute Dye Solutions", App. Spectro., **48**, 400-405,1994

[25] S. Teukolsky W. Press, W. Vetterling, B. Flannery, "Direction Set (Powell's) Methods in Multidimensions", Numerical Recipes in C, 412-420,1995

[26] M. Leiner P. Hartmann, M. Lippitsch, "Response characteristics of luminescent oxygen sensors", sens. actu. B, **29**, 251-257,1995

[27] E. Austin and J. Dakin, Simultaneous sensing of dissolved oxygen and probe-tip temperature, using a ruby insert and compact photon counting receiver (postdeadline paper), *OFS 13*, 2000

[28] Z. Xu S. Liao, J. Izatt, J. Alcala, "Real-Time Frequency Domain Temperature and Oxygen Sensor with a SIngle Optical Fiber", IEEE. Trans. Bio. Eng., **44**, 1114-1121,1997

[29] E. Austin, J. Dakin and A.P Strong, Use of transition-metal-doped sapphire crystals to calibrate and thermally compensate fluorescent-lifetime chemical detectors (keynote communication), *EUROPT(R)ODE V*, 2000

[30] E. Austin and J. Dakin, Recent measurements with Ru2+ oxygen sensors, using doped sapphire crystals, both as a calibration aid and an integral temperature sensor (invited paper), *Fiber Optic Sensor Technology II*, 4204, SPIE, 2000